Numerical and Dynamic Features for Heat Transfer Through a Longitudinal Rectangular Fin with Temperature-Dependent Thermal Conductivity

OKEY OSELOKA ONYEJEKWE
Robnello Unit for Continuum Mechanics and Nonlinear Dynamics, Umuagu, Oshimili South, Asaba Delta State, NIGERIA

Abstract In the work reported herein, we adopt a Newton-Richtmeyer iterative scheme to arrive at solutions describing heat transfer in a longitudinal rectangular fin. Both the thermal conductivity and heat transfer coefficients are assumed to be temperature dependent and the governing partial differential equation highly nonlinear. In order to validate the numerical formulation, we consider some analytical results for this class of problems at steady state .Comparisons show convergence to exact solutions as demonstrated by local and global error indicators. In addition,various fin parameters which play a key role for efficient fin operation and design are investigated by carrying out a comprehensive dynamical qualitative study.

Keywords: longitudinal fin, nonlinear, partial differential equation, Newton-Richtmeyer scheme, numerical, analytical, qualitative study

Received: September 26, 2022. Revised: August 28, 2023. Accepted: September 19, 2023. Published: October 31, 2023.

1. Introduction

Many significant phenomena in continuum physics are nonlinear; and defy closed form or analytical solutions except in a few cases [1]-[3]. For nonlinear problems, many numerical approaches usually linearize the governing differential equation before applying iterative procedures built around numerical approximations. Variations of thermal conductivity in fins and the accompanying nonlinearity for these types of models have been extensively studied [4]-[8]. Progress in this field, is reflected by the development of the so called semi-exact analytical techniques or hybrid numerical and analytic techniques [9-12]. The homotopy analysis method (HAM) is a utilitarian approximate analytic technique used for obtaining solutions for strongly nonlinear problems [12]. The choice of some initial approximations and auxiliary linear operators facilitates the conversion of a complicated nonlinear differential equation into an infinite number of linear sub-problems which are finally handled by summation.

A lot of work involving the application of optimization techniques to nonlinear fin problems has been ongoing in literature. We refer the reader to [13]-[15]. Further efforts include applications to annular fins [16]-[17]. More recently formulations involving function approximating ability of Legendre polynomials based on artificial neural networks (ANN) have come into the picture. These comprise the global search optimization ability of Whale optimization algorithm (WOA), and local search convergence technique of Nelder-Mead algorithm [18].

Most of these methods , especially semi-analytic techniques can provide reliable results only when the nonlinearities are weak. Apart from involving complex mathematical analysis, they are also encumbered by relatively large number of terms, and implicit expressions which

oftentimes involve rigorous computations. Hence they have not been found useful in large scale design and analysis. On the other hand domain based numerical techniques like the finite element FEM) and especially finite difference methods (FDM), have been widely applied with significant success to transient nonlinear problems. While the FEM relies on the characterization of the governing boundary value equations by minimization principle involving integral equations, FDM is more straightforward, and less complicated [19]-[21].

In this work we deploy an implicit finite difference Newton-Richtmeyer scheme to compute the one- dimensional, nonlinear, heat transfer process in a longitudinal rectangular fin with temperature dependent thermal properties. In addition, we carry out a qualitative study in order to investigate how the solution behaves for various parameter changes. Subtle changes, produce different trajectories of the given system known as phase planes. The shape of these paths, the direction of the trajectories and their characterizations close to the critical points are the essential features of this approach. Except for [22] this approach has often been neglected .

2. Mathematical Formulation

We consider a rectangular longitudinal one dimensional fin with cross-sectional area A_c. Fin perimeter is given by P, and the length denoted by L. The fin is attached to a fixed base of temperature T_b and extends into a fluid whose temperature is denoted by T_a. From conservation of energy, the governing equation for the heat transfer process in the fin is given as:

$$\rho c_v \frac{\partial T}{\partial t} = A_c \frac{\partial}{\partial X}\left(K(T)\frac{\partial T}{\partial X} \right) - PH(T)(T - T_a) \quad (1)$$

where K and H are non-uniform thermal conductivity and heat transfer coefficient and are both dependent on temperature . We adopt the procedure in [23] for nondimentionalization of equation (1).

$$H(T) = h_b \left(\frac{T - T_a}{T_a - T_b} \right)^n ,$$

$$K(T) = k_a \left[1 + \beta (T - T_a) \right]$$

where β is the thermal conductivity parameter, T_a is the ambient temperature, k_a is the thermal conductivity of the fin at ambient temperature, h_b is the fin temperature coefficient at fin base, ρ is the density, n , the convective heat transfer power, is an exponent that accounts for the heat transfer mode ranging from nucleate boiling to thermal radiation, c_v is the volumetric heat capacity, T is the temperature, t is the time variable while X is the spatial coordinate. Equation (1) is a transient, one- dimensional, nonlinear partial differential equation. To be tractable numerically, it requires initial and boundary conditions. Initially, the fin is kept at the temperature of the fluid (the ambient temperature).

$$T(0, X) = T_a \quad (2)$$

The model problem is specified in such a way that at the fin base a temperature is specified explicitly, while there is insulation at the other end. This situation admits a Dirichlet and Neumann types of boundary conditions given as:

$$T(t, L) = T_b \qquad and \qquad \left. \frac{\partial T}{\partial X} \right|_{x=0} = 0 \quad (3)$$

In order to further facilitate the numerical solution of the model equations, we introduce the following dimensionless variables:

$$\xi = \frac{X}{L}, \tau = \frac{k_a t}{\rho c_v L^2}, \theta = \frac{T - T_a}{T_b - T_a},$$
$$k = \frac{K}{k_a}, h = \frac{H}{h_b}, \psi^2 = \frac{2Ph_b L^2}{A_c k_a},$$
$$\beta = \lambda(T - T_\alpha) \quad (4)$$

These reduce equation (1) into the following dimensionless form

$$\frac{\partial \theta}{\partial \tau} = \frac{\partial}{\partial \xi}\left(k(\theta)\frac{\partial \theta}{\partial \xi}\right) - \psi^2 \theta h(\theta),\ 0 < \xi < 1 \quad (5)$$

$\xi, \tau, \theta, h(\theta), k(\theta), \psi$ are defined as dimensionless distance, time, temperature, heat transfer coefficient, thermal conductivity and thermo-geometric fin parameter respectively. For practical purposes, the heat transfer coefficient is often chosen as a power law representation of the temperature variable; $h(\theta) = \theta^n$, where n is the power law coefficient of the heat transfer variable and for practical purposes takes on values within the range of $-3 \prec n \succ 3$. For this study the thermal conductivity varies linearly with temperature and is given as $k(\theta) = (1 + \beta(\theta))$, where, $\beta = \lambda(T_b - T_a)$ and λ is a measure of thermal conductivity heat with temperature. Equation (5) can now be recast to read

$$\frac{\partial \theta}{\partial \tau} = \frac{\partial}{\partial \xi}\left(\left[1 + \beta(\theta)\right]\frac{\partial \theta}{\partial \xi}\right) - \psi^2 \theta^{n+1}$$
$$0 \prec x \prec 1 \quad (6)$$

where the thermal conductivity parameter β is non-zero. The associated initial and boundary conditions of equation (6) are restated as follows:

$$\theta(0, \xi) = 0,\ \theta(\tau, 1) = 1,\ \left.\frac{\partial \theta}{\partial \xi}\right|_{x=0} = 0$$
$$\tau \geq 0 \quad (7)$$

3. Newton-Richtmyer scheme

To allow for a more robust treatment, equation (6) is represented generically as

$$\left(\frac{\partial \theta}{\partial t}\right)_i^k = (1 - \lambda)\left[\frac{\partial}{\partial \xi}\left(\alpha(\theta)\frac{\partial \theta}{\partial \xi}\right) + f(\theta)\right]_i^k + \lambda\left[\frac{\partial}{\partial \xi}\left(\alpha(\theta)\frac{\partial u}{\partial \xi}\right) + f(\theta)\right]_i^{k+1} \quad (8)$$

where $\alpha(u)$ $f(u)$ represent nonlinear conduction and sink terms. Equation (8) is represented implicitly as:

$$\left(\frac{\partial \theta}{\partial t}\right)_i^k = \left[\frac{\partial}{\partial \xi}\left(\alpha(\theta)\frac{\partial \theta}{\partial \xi}\right) + f(\theta)\right]_i^{k+1} \quad (9)$$

Where k is the notational time variable for old and new time steps. The RHS is key to the development of this scheme in the sense that if it signifies the ***new*** values, then it is proper we have an idea of what the ***old*** values are in the first place. We initiate this procedure, by considering one of the terms in the bracket $\left(\alpha(\theta)\frac{\partial \theta}{\partial \xi}\right)$. For the purposes of this analysis we refer to it as the ***pseudo convection*** term and is expressed as:

$$\left(\alpha\frac{\partial \theta}{\partial \xi}\right)_i^{k+1} \approx \underbrace{\left(\alpha\frac{\partial \theta}{\partial \xi}\right)_i^k}_{First\ Term} + \Delta t \underbrace{\left[\partial/\partial t\left(\alpha\frac{\partial \theta}{\partial \xi}\right)\right]_i^k}_{Second\ Term} \quad (10)$$

Applying the product rule of derivatives on the *second term* of equation (10) yields:

$$\left(\alpha\frac{\partial\theta}{\partial\xi}\right)_i^{k+1} \approx \left(\alpha\frac{\partial\theta}{\partial\xi}\right)_i^{k} + \Delta t\left[\alpha_i^k\left(\partial^2\theta/\partial\xi\partial t\right)_i^k + \left(\partial\alpha/\partial t\right)_i^k\left(\partial\theta/\partial\xi\right)_i^k\right] \quad (11)$$

Hence

$$\left(\alpha\frac{\partial\theta}{\partial x}\right)_i^{k+1} \approx \left(\alpha\frac{\partial\theta}{\partial x}\right)_i^{k} + \Delta t\left[\alpha_i^k\frac{\partial}{\partial x}\left(\frac{\partial\theta}{\partial t}\right)_i^k + \left(\partial\alpha/\partial\theta\right)_i^k\left(\partial\theta/\partial t\right)_i^k\left(\frac{\partial\theta}{\partial x}\right)_i^k\right] \quad (12)$$

The temporal term in equation (9) is simply approximated with a forward difference scheme:

$$\left(\frac{\partial\theta}{\partial t}\right)\Big|_i^k = \frac{\theta_i^{k+1}-\theta_i^k}{\Delta t} = \frac{\Delta\theta_i^{k+1}}{\Delta t} \quad (13)$$

Introduce equation (13) into (12) to yield:

$$\left(\alpha\frac{\partial\theta}{\partial\xi}\right)_i^{k+1} \approx \left(\alpha\frac{\partial\theta}{\partial\xi}\right)_i^{k} + \left[\alpha_i^k\frac{\partial}{\partial\xi}(\Delta\theta)_i^{k+1} + \left(\partial\alpha/\partial\theta\right)_i^k\left(\frac{\partial\theta}{\partial\xi}\right)_i^k(\Delta\theta)_i^{k+1}\right] \quad (14)$$

or

$$\left(\alpha\frac{\partial\theta}{\partial\xi}\right)_i^{k+1} \approx \left(\alpha\frac{\partial\theta}{\partial\xi}\right)_i^{k} + \alpha_i^k\frac{\partial}{\partial\xi}(\Delta\theta)_i^{k+1} + \left(\partial\alpha/\partial\theta\right)_i^k\left(\frac{\partial\theta}{\partial\xi}\right)_i^k(\Delta\theta)_i^{k+1} \quad (15)$$

The RHS of equation (9) can be written as:

$$\left(\frac{\partial}{\partial x}\left(\alpha\frac{\partial\theta}{\partial x}\right)+f(\theta)\right)_i^{k+1} \approx \frac{\partial}{\partial x}\left[\begin{array}{l}\left(\alpha\frac{\partial\theta}{\partial x}\right)_i^k + \alpha_i^k\frac{\partial}{\partial x}(\Delta\theta)_i^{k+1} + \\ \left(\partial\alpha/\partial\theta\right)_i^k\left(\frac{\partial\theta}{\partial x}\right)_i^k(\Delta\theta)_i^{k+1}\end{array}\right] + \left(f(\theta)\right)_i^{k+1} \quad (16)$$

Now we substitute equation (16) into equation (9) to give:

$$\left(\frac{\partial\theta}{\partial t}\right)_i^k = \overbrace{\frac{\partial}{\partial\xi}\left[\left(\alpha\frac{\partial\theta}{\partial\xi}\right)_i^k + \alpha_i^k\frac{\partial}{\partial\xi}(\Delta\theta)_i^{k+1} + \left(\partial\alpha/\partial u\right)_i^k\left(\frac{\partial\theta}{\partial\xi}\right)_i^k(\Delta\theta)_i^{k+1}\right] + f(\theta)_i^{k+1}}^{} \quad (17)$$

The derivative terms are approximated discretely a

$$(\Delta\theta)_i^{k+1} = \theta_i^{k+1} - \theta_i^k \quad (18a)$$

$$\left(\frac{\partial\theta}{\partial x}\right)_{i+1/2}^k = \frac{\left(\theta_{i+1}^k - \theta_i^k\right)}{\Delta\xi} \quad (18b)$$

$$\left(\frac{\partial\theta}{\partial t}\right)_i^{k+1} = \frac{\left(\theta_i^{k+1} - \theta_i^k\right)}{\Delta t} = \frac{(\Delta\theta)_i^{k+1}}{\Delta t} \quad (18c)$$

$$\left(\frac{\partial\theta}{\partial x}\right)^{k}_{i-1/2} = \frac{\left(\theta_i^k - \theta_{i-1}^k\right)}{\Delta\xi} \qquad (18d)$$

$$\left(\Delta\theta\right)^{k+1}_{i+1/2} = \frac{\left(\Delta\theta_{i+1}^{k+1} + \Delta\theta_i^{k+1}\right)}{2} \qquad (18e)$$

$$\left(\Delta\theta\right)^{k+1}_{i-1/2} = \frac{\left(\Delta\theta_i^{k+1} + \Delta\theta_{i-1}^{k+1}\right)}{2} \qquad (18f)$$

Further simplification yields :

$$\Delta\theta_i^{(k+1)} = \Delta t\left[\frac{\lambda(\alpha)^k_{i+1/2}\left(\theta_{i+1}^k - \theta_i^k\right) - \lambda(\theta)^k_{i-1/2}\left(\theta_i^k - \theta_{i-1}^k\right)}{\Delta\xi^2}\right] +$$
$$\Delta t\left[\frac{\lambda(\alpha)^k_{i+1/2}\left(\Delta\theta_{i+1}^{k+1} - \Delta\theta_i^{k+1}\right) - \lambda(\alpha)^k_{i-1/2}\left(\Delta\theta_i^{k+1} - \Delta\theta_{i-1}^{k+1}\right)}{\Delta\xi^2}\right] +$$
$$\Delta t\left[\frac{\lambda\left(\frac{\partial\alpha}{\partial u}\right)^k_{i+1/2}\left(\theta_{i+1}^k - u_i^k\right)\left(\Delta\theta_{i+1}^{k+1} - \Delta\theta_i^{k+1}\right) - \lambda\left(\frac{\partial\alpha}{\partial u}\right)^k_{i-1/2}\left(\theta_i^k - u_{i-1}^k\right)\left(\Delta\theta_i^{k+1} - \phi u_{i-1}^{k+1}\right)}{2\Delta\xi^2}\right] +$$
$$\Delta t\left[\frac{(1-\lambda)(\alpha)^k_{i+1/2}\left(\theta_{i+1}^k - \theta_i^k\right) - (1-\lambda)(\alpha)^k_{i-1/2}\left(\theta_i^k - \theta_{i-1}^k\right)}{\Delta\xi^2}\right] +$$
$$\Delta t\left[\left(f(\theta)\right)_i^k + \left(\frac{\partial f}{\partial u}\right)_i^k (\theta_i^{k+1})\right]$$

(19)

The Newton-Richtmeyer scheme has been adopted to carry out linearization involving the nonlinear source and the conduction terms. The resulting equation (19) is in ***delta form*** $\left(\Delta u\right)_i^{(k+1)}$. And t can be expressed in a tridiagonal matrix form as

$$A_i^{(k)}\Delta\theta_{i-1}^{k+1} + B_i^{(k)}\Delta\theta_i^{k+1} + C_i^{(k)}\Delta\theta_{i+1}^{k+1} = D_i^k \quad (20)$$

The discrete analog of the governing differential equation

after some non-trivial algebra is given as

where A, B, and C are coefficients of the tri-diagonal matrix and D the 'known' ing to equation (20). Let $r = \Delta t/\Delta\xi^2$, then

DOI: 10.37394/232026.2023.5.14

$$A_i^j = -\lambda\left[(r)\{\alpha\}_{i-1/2}^k - (r/2)\{\partial\alpha/\partial\theta\}_{i-1/2}^k * \{\theta_i^k - \theta_{i-1}^k\}\right]$$

$$B_i^j = \left[1.0 + \lambda(r)\left(\{\alpha\}_{i+1/2}^k + \{\alpha\}_{i-1/2}^k\right) - \lambda(r/2)\begin{pmatrix}\{\partial\alpha/\partial\theta\}_{i+1/2}^k * \{u_{i+1}^k - u_i^k\} + \\ \{\partial\alpha/\partial\partial\}_{i-1/2}^k * \{\theta_i^k - \theta_{i-1}^k\}\end{pmatrix} - \lambda\Delta t\left(\frac{\partial f}{\partial u}\right)_i^k\right]$$

$$C_i^j = -\lambda\left[(r)\{\alpha\}_{i+1/2}^k + (r/2)\{\partial\alpha/\partial\theta\}_{i+1/2}^k * \{\theta_{i+1}^k - \theta_i^k\}\right]$$

$$D_i^j = \left[(r)\{\alpha\}_{i+1/2}^k * \{\theta_{i+1}^k - \theta_i^k\} - (r)\{\alpha\}_{i+1/2}^k * \{\theta_i^k - \theta_{i-1}^k\} + \Delta t\left(f(\theta)_i^k\right)\right]$$

(21)

The dependent variable is finally obtained as :

$$\theta(\xi_i, t_{k+1}) = \theta(\xi_i, t_k) + \Delta\theta(\xi_i, t_k) \quad (22)$$

3. Results and Discussion

3. 1 Linear Case

We convert equation (6) to steady-state and test for linear and nonlinear scenarios in order to facilitate comparison with available literature results.

When $\frac{\partial\theta}{\partial\tau} = 0, \quad \beta = 0, n = 0$; equation (6) becomes time invariant and linear. The thermal conductivity parameter is no longer under consideration. Together with the boundary conditions; the analytical solution is:

$$\theta(x) = \frac{\cosh(\psi x)}{\cosh(\psi)} \quad (23)$$

Tables (1) and (2) are in excellent agreement with those shown in [24] for the same fin parameters.

DOI: 10.37394/232026.2023.5.14

Table 1 : Linear Solution for $\psi = 0.5$

$\beta = 0$					
X	$\psi = 0.5$ *current*	$\psi = 0.5$ *Exact*	$\psi = 0.5$ *LMM*	$\psi = 0.5$ *HAM*	$\psi = 0.5$ *DTM*
0.00	0.886819	0.88681	0.886819	0.88681	0.88681
0.05	0.887096	0.88709	0.887096	0.887096	0.88709
0.10	0.887928	0.88792	0.887928	0.88792	0.88792
0.15	0.889314	0.88931	0.889314	0.88931	0.88931
0.20	0.891257	0.89125	0.891257	0.89125	89125
0.25	0.893756	0.89375	0.893756	0.89375	0.89375
0.30	0.896814	0.89681	0.896814	0.89681	0.89681
0.35	0.900433	0.90043	0.900433	0.90043	0.90043
0.40	0.904614	0.90461	0.904614	0.90461	0.90461
0.45	0.909361	0.90936	0.909361	0.90936	0.90936
0.50	0.914677	0.91467	0.914677	0.91467	0.91467
0.55	0.920564	0.92056	0.920564	0.92056	0.92056
0.60	0.927026	0.92702	0.927026	0.92702	0.92702
0.65	0.934068	0.93406	0.934068	0.93406	0.93406
0.70	0.941693	0.94169	0.941693	0.94169	0.94169
0.75	0.949907	0.94990	0.930411	0.94990	0.94990
0.80	0.958715	0.95871	0.958715	0.95871	0.95871
0.85	0.968123	0.96812	0.968123	0.96812	0.96812
0.90	0.978135	0.97813	0.978135	0.97813	0.97813
0.95	0.988758	0.98875	0.988758	0.98875	0.98875
1.00	1.000000	1.000000	1.000000	1.000000	1.000000

DOI: 10.37394/232026.2023.5.14

Table 2: Linear Solution for $\psi = 1.0$

$\beta = 0$					
X	$\psi = 1.0$ *Current*	$\psi = 1.0$ *Exact*	$\psi = 1.0$ *LMM*	$\psi = 1.0$ *HAM*	$\psi = 1.0$ *DTM*
0.00	0.648054	0.64805	0.648054	0.64805	0.64805
0.05	0.648865	0.64886	0.648865	0.64886	0.64886
0.10	0.651297	0.65129	0.651297	0.65129	0.65129
0.15	0.665359	0.65535	0.665359	0.65535	0.65535
0.20	0.661059	0.66105	0.661059	0.66105	0.66105
0.25	0.668412	0.66841	0.668412	0.66841	0.66841
0.30	0.677436	0.67743	0.677436	0.67743	0.67743
0.35	0.688154	0.68815	0.688154	0.68815	0.68815
0.40	0.700594	0.70059	0.700594	0.70059	0.70059
0.45	0.714785	0.71478	0.714785	0.71478	0.71478
0.50	0.730763	0.73076	0.730763	0.73076	0.73076
0.55	0.748568	0.74856	0.748568	0.74856	0.74856
0.60	0.768246	0.76824	0.768246	0.76824	0.76824
0.65	0.789844	0.78984	0.789844	0.78984	0.78984
0.70	0.813418	0.81341	0.813418	0.81341	0.81341
0.75	0.839025	0.83902	0.839025	0.83902	0.83902
0.80	0.866730	0.86670	0.866730	0.86670	0.86670
0.85	0.896603	0.89660	0.896603	0.89660	0.89660
0.90	0.928718	0.92871	0.928718	0.92871	0.92871
0.95	0.963155	0.98875	0.963155	0.98875	0.98875
1.00	1.000000	1.000000	1.000000	1.000000	1.000000

DOI: 10.37394/232026.2023.5.14

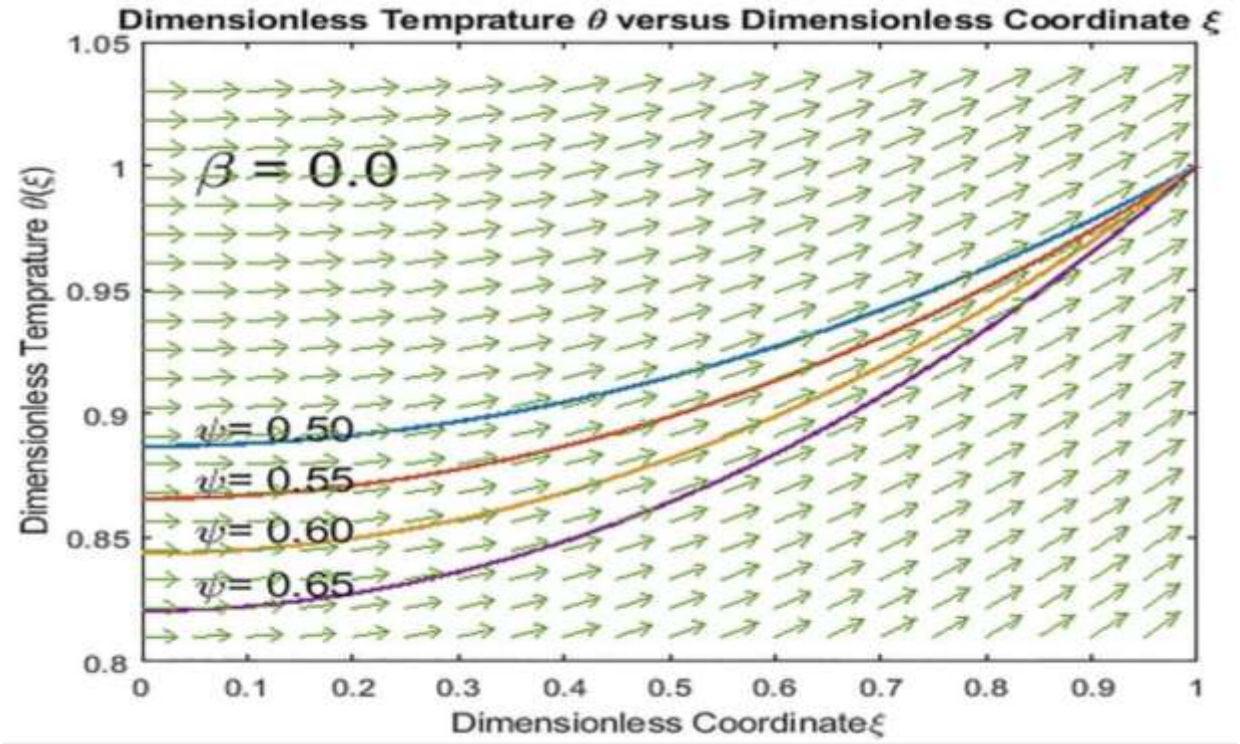

Figure 1: Linear Solution for various values of ψ

Fig. 1 displays the temperature profiles for the linear solution. It can be observed that larger values of the thermogeometric parameter ψ , produce higher temperature profile gradients. This is in consonance with the definition of ψ as found in equation (4). Assuming we keep to the same geometric characteristics for all the runs, higher values of ψ results in higher convection at the base of the fin or lower heat conductivity.

DOI: 10.37394/232026.2023.5.14

3. 2 Nonlinear Case $(\beta \neq 0)$

Results obtained from the steady state analog of the governing differential equation allows for direct comparison with those found in literature .

$$\frac{d^2\theta}{dx^2} = \frac{-\beta}{(1+\beta\theta)}\left(\frac{d\theta}{dx}\right)^2 + \frac{\psi^2\theta^{(n+1)}}{(1+\beta\theta)} \qquad (24)$$

where $D(\theta) = (1+\beta\theta)$; it follows that :

$$\frac{d^2\theta}{d\xi^2} = \left(\frac{-d\left(\ln D(\theta)\right)}{d\xi}\right)\left(\frac{d\theta}{dx}\right) + \frac{\psi^2\theta^{(n+1)}}{D(\theta)} \qquad (25)$$

where

$$\frac{-\beta}{(1+\beta\theta)}\left(\frac{d\theta}{d\xi}\right)^2 = \left(\frac{-\beta}{(1+\beta\theta)}\left(\frac{d\theta}{d\xi}\right)\right)\left(\frac{d\theta}{d\xi}\right) = \left(\frac{-d\left(\ln D(\theta)\right)}{d\xi}\right)\left(\frac{d\theta}{d\xi}\right) \qquad (26)$$

We compare numerical results obtained by solving equation (24) with those solved by Leibnitz-MacLaurin's method (LMM) and the homotopy analysis method (HAM) [24]. Table 3 confirms the closeness of the results for all the cases tested. Overall, the results of the tests not only satisfy the boundary conditions but also confirm the validity of the problem formulation.

DOI: 10.37394/232026.2023.5.14

Table 3: Nonlinear Solution for various values of β

x	$\beta = 0.2$ *Current*	$\beta = 0.2$ *LMM*	$\beta = 0.2$ *HAM*
0.00	0.903447	0.903447	0.90344
0.05	0.903687	0.903686	0.90348
0.10	0.904405	0.904404	0.90440
0.15	0.905600	0.905599	0.90559
0.20	0.907277	0.907276	0.90727
0.25	0.909431	0.909429	0.90942
0.30	0.912064	0.912063	0.91206
0.35	0.915179	0.915178	0.91517
0.40	0.918776	0.918774	0.91877
0.45	0.922853	0.922853	0.92285
0.50	0.927416	0.927416	0.92741
0.55	0.932466	0.932464	0.93246
0.60	0.93800	0.937998	0.93799
0.65	0.944023	0.944021	0.94402
0.70	0.950533	0.950533	0.95053
0.75	0.957538	0.957537	0.95753
0.80	0.965033	0.965034	0.96503
0.85	0.973026	0.973026	0.97302
0.90	0.981516	0.981517	0.98151
0.95	0.990505	0.990507	0.99050
1.00	1.0000	1.0000	1.0000

DOI: 10.37394/232026.2023.5.14

To further confirm the numerical accuracy of this work, dimensionless temperature profiles for different values of fin parameters are investigated.

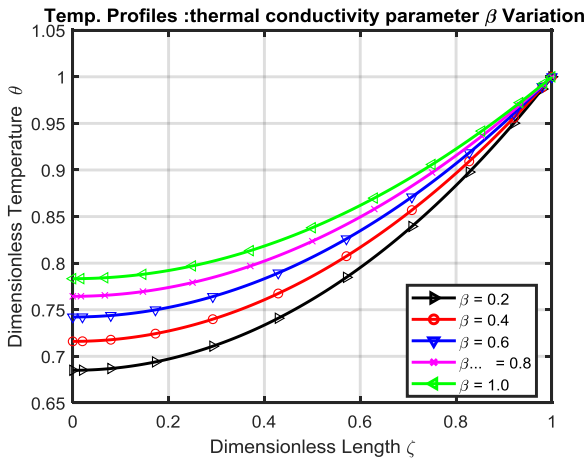

Fig. 2 Dimensionless temperaure profiles for β variation ,

$n = 0,\ \psi = 1$

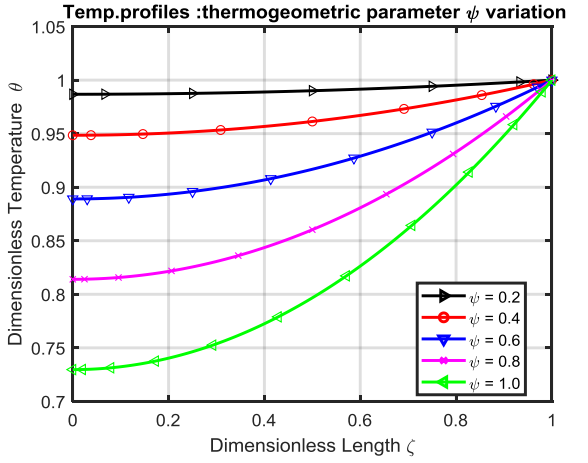

Fig. 3 Dimensionless temperaure profiles for ψ variation , $n = 0,\ \beta = 0.5$

As expected, Fig. 2 shows that higher values of conduction parameter β yield higher magnitudes of temperature. On the other hand, higher values of thermo-geometric fin parameter ψ produce lower temperatures (fig.3) (see equation 4).

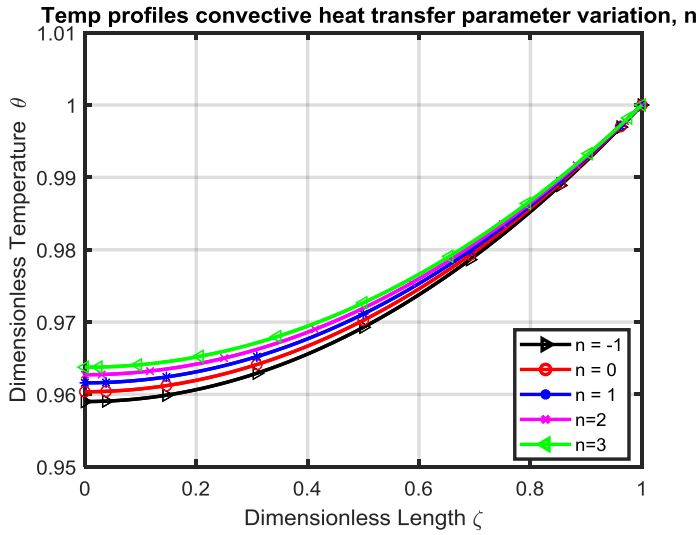

Fig. 4 Dimensionless temperture profiles for convective heat transfer parameter

(n) variation, $\beta = 0.1,\ \psi = 0.3$

Fig.4 displays the effect of different values of the convective heat transfer parameter 'n' on the dimensionless temperature profiles . The typical heat transfer modes for different fin operations covers a considerable portion of fin heat transfer operation $-6.6 \le n \ge 5$. However for practical purposes $-3 \le n \ge 3$ is considered , For nucleate boiling, n=2, and n =3 .

For radiation and constant heat transfer n=0 [21]. Higher values of the parameter 'n' facilitates convection. This basically explains the shapes of the profiles.

The effect of an increase of the thermal conductivity parameter β, on the dimensionless temperature profiles, keeping all the other parameters the same is shown in Fig. 5. As can be seen, higher temperatures were recorded for all values of n considered. Higher values of the parameter β facilitates conduction and according to its definition, implies higher differences between the temperature at the base of the fin and the ambient.

Fig. 6 shows a reverse change in temperature for an increase in the thermogeometric parameter ψ. Higher ψ value, results in lower conductivity assuming that the geometery of the fin is kept constant.

On the whole, the overall shapes of the profiles for the various fin parameters considered are in consonance with the fin differential equation.

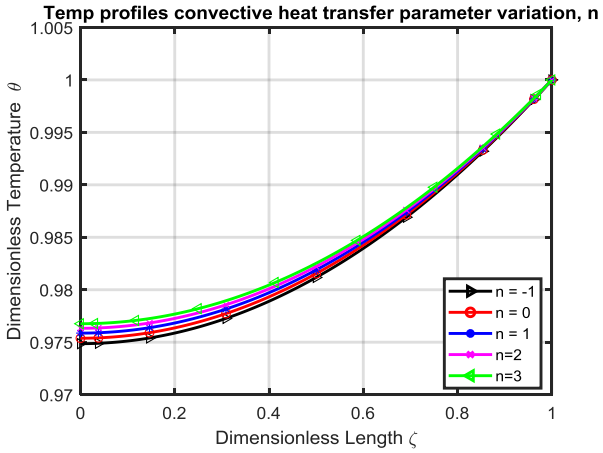

Fig5 Dimensionless temperture profiles for convective heat transfer parameter (n) variation, $\beta = 0.8, \psi = 0.3$

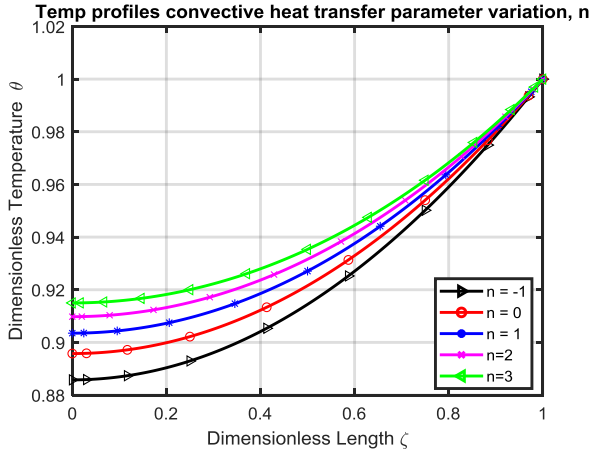

Fig. 6 Dimensionless temperture profiles for convective heat transfer parameter 'n' variation, $\beta = 0.1, \psi = 0.5$

The significance of these computations are further enhanced by relating them to fin efficiency η.

Assuming the total length of the fin is at the same temperature as that at the base, and the fin efficiency is defined as the ratio of

the actual heat rate through the fin base to the ideal heat flow, then

$$\eta = \frac{Q_f}{Q_{\max}} = \frac{\int_0^L Ph\left(T - T_\infty\right) dx}{PLh_b\left(T_b - T_\infty\right)} = \int_0^1 \theta^{(n+1)} d\xi \quad (27)$$

Table 4 shows that lower fin efficiencies are recorded for an increase in ψ for various fin heat transfer modes for a fixed value of $\beta = 0.1$. On the other hand , column 2 of Table 4 shows a relatively higher value of efficency when β is increased. The reason for this is not far fetched. A relatively low efficiency,implies a high $Q_{\max}$ or a high heat transfer coefficient h_b a t the base of the fin. In either case, the difference between the temperature of the fin base and the ambient is high as well. Assuming the fin geometry is kept contant, a high value of thermogeometric parameter will correspond to a high value of heat transfer coefficent at the fin base.

Table 4 Efficiency for changes in fin parameters for different heat transfer modes

n values	efficiency η $\beta = 0.1,\ \psi = 0.3$	efficiency η $\beta = 0.8, \psi = 0.3$	efficiency η $\psi = 0.5, \beta = 0.1$
0	0.9736	0.9836	0.9303
1	0.9495	0.9681	0.8756
2	0.9274	0.9535	0.8306
3	0.9070	0.9396	0.7931

Fig.7 displays the total heat flux q_T

at nucleate boiling $(n = 2)$

for different Biot numbers. It is given in [25] as

$$q_T = \frac{1}{Bi}\frac{k(\theta)}{h(\theta)}\frac{d\theta}{d\xi} = \frac{1}{Bi}(1 + \beta\theta)\theta^{-n}\frac{d\theta}{d\xi} \qquad (28)$$

The higher the Biot numbers the lower the q_T. The relative importance of conduction and convection with regards to the total heat flux at the base of the fin is confirmed by the shapes of the profiles. As can be observed, lower values of Biot number indicate that the conductive resistance of the fin is comparatively lower than its external resistance.

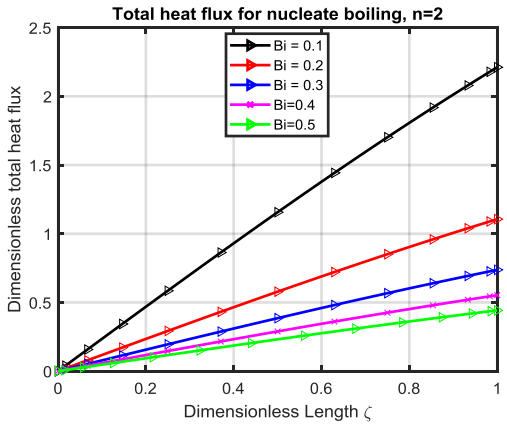

Fig. 7 Total heat flux q_T at nucleate boiling $(n=2)$ for Biot number variation $(\psi=0.5,\ \beta=0.5)$

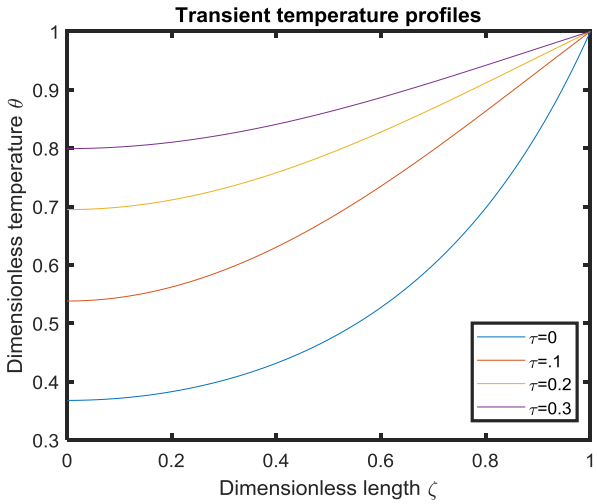

Fig. 8a Transient temperature profiles for $\psi=0.1,\ \beta=0.5,\ n=0$

Figs 8a and 8b show the dimensionless transient temperature histories for different fin parameter values. There is progress towards steady state as dimensionless time τ increases. The dimensionless temperature profiles are in conformity with our earlier observation for steady state solution (see fig. 4).

DOI: 10.37394/232026.2023.5.14

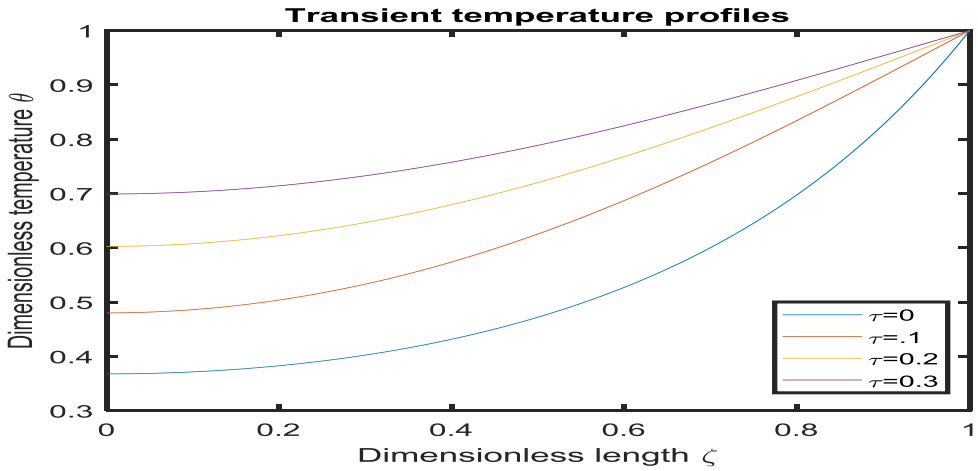

Fig.8b Transient temperature profiles

for $\psi = 0.1,\ \beta = 0.1,\ n = 0$

4. Qualitative Analysis

A better insight into fin operation and design can be obtained by implementing a dynamical analysis in a phase space. By so doing, we can visually appreciate the dynamically changing behavior of a system in the vicinity of points of equilibrium. This offers a less costly avenue of gaining an insight into the systems performance which otherwise would have been very difficult to obtain by solving the governing differential equations via a different route. Not only are meaningful references obtained for design purposes, the effects of certain parameters which significantly influence fin operation can also be identified.

If for example a nonlinear system of differential equations possesses an equilibrium, the dynamical behavior of the orbits in the vicinity of that point is displayed by a linear system obtained by getting rid of the nonlinear terms. The eigenvalues of the associated linear system provide further insight related to the properties of the nonlinear sytem. This approach which is often referred to as qualitative analysis or *local stability analysis* is fast becoming a reliable method for obtaining the general behavior of solutions depending on their initial conditions.

We demonstrate this procedure by rewriting Equation (24) as a system of first-order ordinary differential equations through the transformations $y_1 = \theta, \quad y_2 = \theta'$ which in turn yield $y_1' = \theta', \quad y_2' = \theta''$. We then arrive at:

$$y_1' = y_2 \qquad (29a)$$

$$y_2' = \frac{1}{(1+\beta y_1)}\left[-\beta (y_2)^2 + \psi^2 y_1\right] \qquad (29b)$$

The fixed points or equilibrium points are points where $y_1^{'} = y_2^{'} = 0$. These yield steady state solutions. For this particular problem, it can straightforwardly be verified that we have a (0, 0) fixed point. To be able to ascertain the nature of this fixed point, we need to linearize the system. The Jacobian matrix is computed as:

$$J(y_1, y_2) = \begin{pmatrix} 0 & 1 \\ \left\{ \dfrac{\psi^2}{(1+\beta y_1)} + \dfrac{\beta\left(\beta y_2^2 - \psi^2 y_1\right)}{(1+\beta y_1)^2} \right\} & \left(\dfrac{-2\beta y_2}{(1+\beta y_1)} \right) \end{pmatrix} \quad (30)$$

The linearization at the equilibrium point is implemented by direct substitution into the Jacobian matrix.

$$J(0,0) = \begin{pmatrix} 0 & 1 \\ \psi^2 & 0 \end{pmatrix} \quad (31)$$

This is followed by the computation of the eigenvalues

$$\begin{pmatrix} -\lambda & 1 \\ \psi^2 & -\lambda \end{pmatrix} = 0 \quad (32)$$

The characteristic equation yields:

$\lambda^2 - \psi^2 = 0 \Rightarrow \lambda = \pm\sqrt{\psi^2} \Rightarrow$

$\lambda_1 = -\psi,\ \lambda_2 = \psi$

Hence the critical point is ***saddle***. The above analyses set the stage for a more robust qualitative analyses using the MATLAB pplane9 software.

There always exists different modes of operations indexed by a parameter whose range of values may be bound by a limit of physical interest. A good example for a fin is the convective heat transfer exponent 'n'. For such cases, dynamical analysis supplements a vague operational information with a visual picture on a plane. In other words, it provides a particular mode of fin operation with a unique identity.

Fig. 9a shows the phase plane sketch of the trajectories. There is a fixed point ***saddle*** at ***critical point*** (0,0) for the following fin parameters: $(\beta = 0.1, \psi = 0.5\ n = 0)$. The computed Jacobian matrix is

$$J = \begin{pmatrix} 0 & 1 \\ 0.01 & -5e-07 \end{pmatrix};$$

The eigenvalues and eigenvectors are

$0.1 \quad (0.99504, 0.99504);$

$-0.1 \quad (-0.99504, 0.99504)$

The eigenvalues are real positive and negative , there are two incoming and outgoing trajectories as well. For the values of fin parameters chosen, this confirms an ***unstable saddle*** close to the critical point.

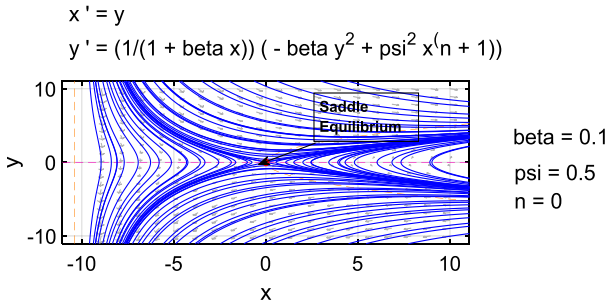

Fig. 9a Phase plane trajectories for the following fin parameters
$\beta = 0.1, \psi = 0.5, \ n = 0$

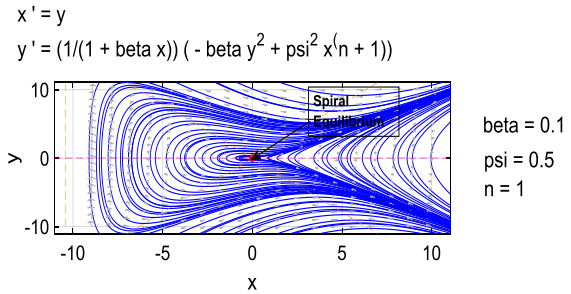

Fig. 9b Phase planr trajectories for the following fin parameters
$\beta = 0.1, \psi = 0.5, \ n = 1$

For Fig. 9b all the fin parameters remain the same but there is an increase in the convective exponent to $'n=1'$. Results for phase plane analysis shows that the ***equilibrium*** is located at $(-0.0073498, 0)$. The following dynamical features are computed:

Jacobian matrix

$$J=\begin{pmatrix} 0 & 1 \\ -0.0001478 & -5.0184e-07 \end{pmatrix}$$

Eigenvalues and eigenvectors

$$-2.5092e-07+0.012157i$$
$$(0.99993, -2.509e-07+0.012156i)$$
$$-2.5092e-07-0.012157i$$
$$(0.99993, -2.509e-07-0.012156i)$$

The dramatic change in phase profiles for an increase in the power exponent in addition to a different characterization of the equilibrium point show how sensitive and important $'n'$is in fin design. The equilibrium point is ***stable spiral sink*** which is characterized by complex eigenvalues with negative real parts.

The next experiment displayed by Fig. 9c, involves a further increase of the convective index to $'n=3'$(radiation mode) while keeping the other fin parameters the same, The ***critical point*** is located at $(-0.02163, 0)$

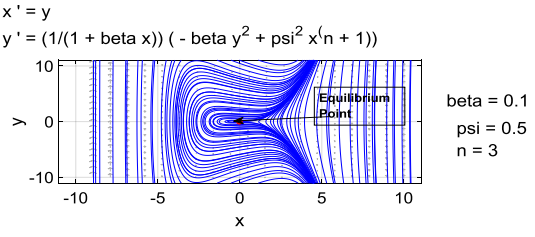

Fig. 9c Dynamical analysis for the following fin parameters
$\beta=0.1,\ \psi=0.5,\ n=3$

The accompanying dynamical features are computed as:

Jacobian matrix

$$J=\begin{pmatrix} 0 & 1 \\ -1.0146e-05 & -1.0022e-07 \end{pmatrix}$$

The eigenvalues and eigenvectors are :

$$-5.0108e-08+0.0031853i$$
$$(0.99999, -5.0108e-08+0.0031853i)$$
$$-5.0108e-08+0.0031853i$$
$$(0.99999, -5.0108e-08+0.0031853i)$$

Again, the behavior near the critical point is that of a ***stable spiral*** . It can be observed that a slight perturbation in the exponent $'n'$ provides sudden changes in the dynamical features of the phase plane profiles . These changes may indicate a close proximity to the death or birth of fixed points , changes in orbits or a tendency towards ***bifurcation***.

5. Conclusion

In the work presented herein, heat transfer in a longitudinal rectangular fin with temperature dependent thermal properties has been analyzed using a Newton-Richtmeyer scheme. The numerical solutions were validated by comparing with steady state exact solutions for the case of the linear problem and by benchmark literature results for the nonlinear problem. Further investigations were carried out to generate transient solution profiles as well as study the effects of various fin heat transfer parameters on temperature profiles. Fin efficiencies for various combinations of fin parameters were also studied to provide valuable information for design. An insight into the dynamical effects of convection power exponent on the numerical solution was carried out with the MATLAB pplane9 software. Changes in the control parameter provided sudden changes in the orbit

structure of the profiles. This may be indicative of an impending ***bifurcation*** .

It is observed that many studies involving engineering design often neglect the phase plane analysis component to the extent that misleading information can often pass unrecognized. Hence careful attention needs to be paid to changes in qualitative behavior. Despite the fact that numerical solutions often display results that are physically realistic, dynamical systems on the other hand can lead to very complex and unpredictable outcomes. It is this realization that has contributed to the groundwork towards efforts that involve comprehensive and better understanding of the universality of the interelatioships among many different branches of science .

It is hoped that this useful trend will continue as computers grow more powerful and the required software becomes more available.

References

[1] R.J. Moitsheki, T. Hayat and M.Y. Malik. Some exact solutions of the fin problem with power law temperature – dependent thermal conductivity, *Nonlinear Analysis: Real World Applications,* Vol. 11 No.5 2010 pp.3287-3294

[2]. S. Abbasbandy and E. Shivanian. Exact closed form solutions to nonlinear model of heat transfer in a straight fin, *International Jnl. Thermal Sciences,* Vol. 116 2017 pp. 45-51

[3]. R.O. Popovycha, C. Sophocleusc, O.O. Vaneeva Exact solutions of a rectangular fin equation, *Appl. Math. Lett.* Vol. 21 2008 pp. 209-214

[4] D. Gupta, P. Saha, S. Ray Computational analysis of perforation effect on the thermo-hydraulic performance of micro-pin fin heat sink *Int. Jnl. Therm. Sci.* 163: 106857, doi: 10.1016/j.ijthermalsci.2021.106857

[5] O.O. Onyejekwe, Simplified integral calculations for radial fins with temperature dependent thermal conductivity, *Jnl. Applied Math and Physics* Vol. 7 2019 pp.513-526

[6] O.O. Onyejekwe, Transient formulations for heat generation fin with a temperature dependent heat transfer coefficient and thermal conductivity, *Advances in Theoretical and Computational Physics,* Vol. 2 2019 pp.1-8

[7] M. Ambarish, C. Gaulam, Improvement of heat transfer through fins: A brief review of recent developments, *Heat Transfer,* Vol. 49, 2020 DOI 10.1002/htj 21684

[8] S. Sundar, R.J. Gireesha, Thermal distribution analysis of rectangular fins considering multiboiling heat transfer modes , https:// doi.org/10.1002/htj.22776 2022

[9]. D.D. Ganji, G.A. Affrouzi and R.A. Talarposhti, Application of variational iteration method and homotopy-perturbation method for nonlinear heat diffusion and heat transfer equations . *Phys. Lett. A.* Vol. 368 2007 No. 6 pp. 450-457

[10]. S.B. Coskun, M.T. Atay. Fin efficiency analysis of convective straight fins with temperature dependent thermal conductivity using variational iteration method *Applied Thermal Engineering* Vol. 28 2008 No. (17-18) pp. 2345-2352

[11]. F. Khani and A. Aziz Thermal analysis of trapezoidal longitudinal fin with temperature -dependent thermal conductivity and heat transfer coefficient .

Communications in in Nonlinear Science and Numerical Simulation Vol. 15 2010 No**.** 3 pp.590-601

[12]. S. J. Liao, On the homotopy analysis method for nonlinear problems *Appl. Math. Comput.* Vol. 147 2004 pp**.** 499-513

[13]. P. Malekzadeh, H. Rahideh, A. R. Setoodeh Optimization of non-symmetric convective radiative annular fin by differential quadrature method , *Energy Convers.. Manage.* Vol. 48 2007 pp**.**1671-1677

[14]. I. Arauzo, C. Cortes, A. Campo Calculation of the optimum dimension of annular fin tube arrays using experimental forced convection coefficents, 3rd European Thermal Science Conference Heidelberg, Allemagne Vol. 10 2003 pp. 1101-1105

[15]. S.M. Zubair, A. Z. Al-Garni, J.S. Nizarmi, The optimal dimensions of circular fins with variable profiles and temperature dependent thermal conductivity, *Int. Jnl. Heat and mass Transf.* Vol. 3 1996 pp. 431-3439

[16]. A. Campo, B. Morone Meshless approach for computing heat liberation from annular fins of tapered cross section, *Appl. Math Comput*. Vol. 156 2004 pp. 137-144

[17]. O.O. Onyejekwe, G. Tamiru, T. Amha, F. Habtamu, Y. Demiss, N. Alemseged, B. Mengistu, Application of an integral numerical technique for a temperature-dependent thermal conductivity fin with internal heat generation, *Journal of Engineering Physics and Thermophysics* , Vol. 93 , 2020 . 1574-1582

[18]. N.A. Khan, M. Sulaiman, P. Kumam, M. A. Bakar, Thermal analysis of conductive-convective-radiative heat exchangers with temperature- dependent thermal conductivity *IEEE Access* Vol. 42016 pp**.**1-30

[19]. G. Nellis , S. Klein, Heat Transfer, Cambridge University Press, New York, Cambridge, Melbourne, Cape Town, Singapore, Sao Paulo, New Delhi 2004

[20]. M. K. Jain, S.R.K. Iyenga, R. K. Jain, Numerical Methods for Numerical and Scientific Computation, 5th Ed. New Age Int. Ltd. 2010

[21]. M.G. Sobamowo Analysis of convective longitudinal fin with temperature-dependent thermal conductivity and internal heat generation , *Alexander Engineering Journal* http://dx.doi.org/10.1016/j.acj.2016.04.022

[22]. C. Harley Asymptotic and dynamical analyses of heat transfer through a rectangular longitudinal fin , *Journal Applied Math.* Article ID 987327, 8 pages, http:// dx.doi.org/10.1155/2013/987327

[23]. R.J. Moitsheki and C. Harley Transient heat transfer in longitudinal fins of various profiles with temperature depdendent thermal conductivity and heat transfer coefficient *Pramana Jnl. Phys.* Vol. 77 2011 pp. 519-532

[24]. P. Mebine, N. Olali Leibnitz-MacLaurin method for solving temperature distribution in straight fins with temperature-dependent thermal onductivity, *Journal of Scientific and Engineering Research,* Vol. 3 No.2,2016 pp. 97-1

Contribution of Individual Authors to the Creation of a Scientific Article (Ghostwriting Policy)

The author contributed in the present research, at all stages from the formulation of the problem to the final findings and solution.

Sources of Funding for Research Presented in a Scientific Article or Scientific Article Itself

No funding was received for conducting this study.

Conflict of Interest

The author has no conflict of interest to declare that is relevant to the content of this article.